Factors Affecting Self-Localization in UHF RFID Tag Networks

YURIY SHMALIY, SANOWAR KHAN
City University London
Dept. of Electronics Engineering
EC1V 0HB, London
UK

OSCAR IBARRA-MANZANO
Universidad de Guanajuato
Dept. of Electronics Engineering
36885, Salamanca
MEXICO

SNUNYI ZHAO
Jiangnan University
Institute of Automation
214122, Wuxi
P.R.CHINA

Abstract: Accuracy of mobile objects self-localization in radio frequency identification (RFID) tag networks depends on many environmental and design factors. This paper analyzes effect of such factors on estimates of the mobile object location. As an estimator, we use the extended finite impulse response (EFIR) filter. It is shown that accuracy of self-localization in the ultra high frequency (UHF) RFID tag networks can be increased by the factor of several times if to optimize design of the tag and network environment and obtain the optimal angle of arrival and viewing angle. Many other factors are also considered.

Key–Words: RFID tag network, self-localization, mobile object, extended FIR filter, extended Kalman filter

1 Introduction

Radio frequency identification (RFID) networking utilizing passive ultra high frequency (UHF) tags has gained currency in self-localization of moving objects [1,2] in recent decades [3]. Each RFID tag has its own identification (ID) number and unique coordinates of location. It may be either active or passive. The passive method is low cost and available for any purpose, provided the communication between an object and the tags. Reviews of RFID tag-based localization algorithms are given in [3–5].

Utilizing received signal strength information (RSSI), the UHF RFID tagging implies measuring distances between an object and several reference tags. The passive UHF RFID tags are "far-field" (long range) devices and their operation is regulated by a global standard [6] in the frequency band of 860–960 MHz. The range for passive UHF RFID tag system is limited by the power of the tag's backscatter [7]. Practically, the range measures up to 10–12 m and the UHF RFID method is fast in data transferring. Although the UHF RFID approach is sensitive to interference, many UHF product manufacturers report that they have found ways of keeping the performance high in diverse environments that is an important advantage against the low frequency (LF) and high frequency (HF) RFID. In 2012, the UHF tag cost was from $\$0.05$ to $\$0.15$ and it follows from technical notes of UHF product manufacturers that the bulk of new projects make UHF RFID the fastest growing segment of the RFID market.

Despite a valuable progress in the UHF RFID technology, the RSSI method commonly does not allow for acceptably accurate localization using multilateration and other "algebraic" algorithms. Therefore, optimal estimators are required, such as the extended Kalman filter (EKF) [8–10], particle filters (PF) [11–13], and extended unbiased finite impulse response (EFIR) filter [14–16].

The EFIR filtering technique [17] demonstrates several critical advantages against the traditional EKF. The EFIR filter completely ignores the noise statistics and initial error statistics [18, 19] which are typically not well known in localization. It is more robust than the EKF in real world under the disturbances and uncertainties peculiar to industrial applications [20, 21]. It is also lesser sensitive to noise [17] and produces smaller round-off errors [21]. Referring to these advantages, the EFIR filter was recently used in [22] to improve the performance of the PF in a hybrid PF/FIR localization structure operating in near realtime. Note that fast operation of PF is typically accompanied with divergence due to impoverishment that cannot be tolerated in the information networks. Although some solutions for the UHF RFID optimization were already addressed in [23–26] and other papers, a lack of systematic investigations still makes it difficult to avoid false focus in obtaining a highest localization accuracy using UHF RFID.

2 Object Model

Consider an object travelling on an indoor floorspace in the RFID tag environment as shown in Fig. 1. An

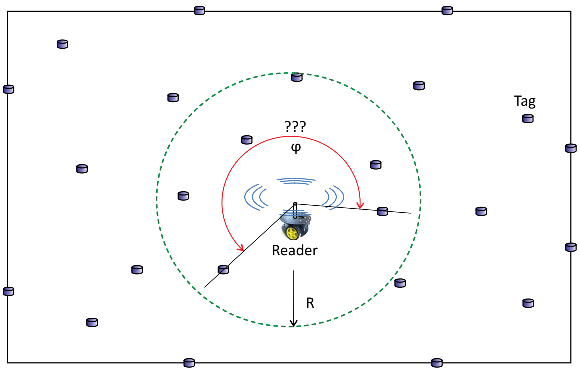

Figure 1: An object (platform) traveling on an indoor floorspace in UHF RFID tag environment.

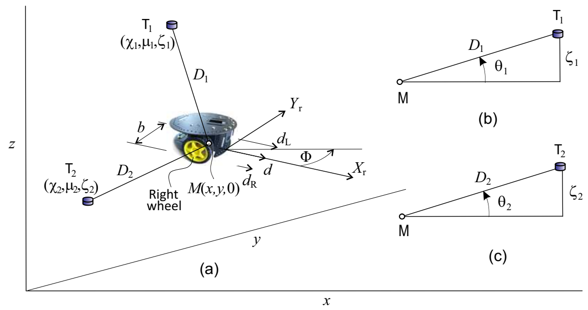

Figure 2: 3D schematic geometry of an object travelling on an indoor floorspace.

object (Fig. 2) travels in direction d and its trajectory is controlled by the left and right wheels. The incremental distances object travels by these wheels are d_L and d_R, respectively. The distance between the left and right wheels is b and the stabilized wheel is not shown. An object moves in its own planar Cartesian coordinates $(X_\mathrm{r}, Y_\mathrm{r})$ with a center at $M(x, y)$. An object is equipped with a fiber optic gyroscope (FOG) which directly measures a pose angle Φ.

At time index n, an object interacts with some k_n tags $\mathrm{T}_t(\chi_t, \mu_t)$, $t \in [1, k_n]$, falling within the reader range (Fig. 1). The tag coordinates (χ_t, μ_t) are precisely known. A case shown in Fig. 2a corresponds to two tags, $\mathrm{T}_1(\chi_1, \mu_1)$ and $\mathrm{T}_2(\chi_2, \mu_2)$ and two distances D_1 and D_2 measured by a reader. Because altitudes are generally different of the points of installation of the reader and the tags, projections to the object plane are calculated following Fig. 2b and Fig. 2c, via the angles of arrival, θ_1 and θ_2. From the object odometry, the incremental distance d_n and the incremental change in heading ϕ_n are provided at discrete time index n by $d_n = \frac{1}{2}(d_{\mathrm{R}n} + d_{\mathrm{L}n})$ and $\phi_n \cong \frac{1}{b}(d_{\mathrm{R}n} - d_{\mathrm{L}n})$.

The state model of an object is nonlinear [14],

$$\mathbf{x}_n = \mathbf{f}_n(\mathbf{x}_{n-1}, \mathbf{u}_n, \mathbf{w}_n, \mathbf{e}_n)\,, \tag{1}$$

where $\mathbf{f}_n = [\, f_{1n}\ f_{2n}\ f_{3n}\,]^T$ has the following components,

$$f_{1n} = x_n \;=\; x_{n-1} + d_n \cos\left(\Phi_{n-1} + \frac{1}{2}\phi_n\right) \tag{2}$$

$$f_{2n} = y_n \;=\; y_{n-1} + d_n \sin\left(\Phi_{n-1} + \frac{1}{2}\phi_n\right) \tag{3}$$

$$f_{3n} = \Phi_n \;=\; \Phi_{n-1} + \phi_n\,, \tag{4}$$

in which the states x_{n-1}, y_{n-1}, and Φ_{n-1} at time $n-1$ are projected to time n by the time-variant incremental distances $d_{\mathrm{L}n}$ and $d_{\mathrm{R}n}$. The states are united in the state vector $\mathbf{x}_n = [\, x_n\ y_n\ \Phi_n\,]^T$ and $\mathbf{u}_n = [\, d_{\mathrm{L}n}\ d_{\mathrm{R}n}\,]^T$ is an input vector of incremental distances. The state noise vector $\mathbf{w}_n = [\, w_{xn}\ w_{yn}\ w_{\Phi n}\,]^T$ and the input noise vector $\mathbf{e}_n = [\, e_{\mathrm{L}n}\ e_{\mathrm{R}n}\,]^T$ have zero mean, $E\{\mathbf{w}_n\} = \mathbf{0}$ and $E\{\mathbf{e}_n\} = \mathbf{0}$, and white Gaussian components with known covariances, $\mathbf{Q} = E\{\mathbf{w}_n\mathbf{w}_n^T\}$ and $\mathbf{L} = E\{\mathbf{e}_n\mathbf{e}_n^T\}$, and $E\{\mathbf{w}_i\mathbf{e}_j^T\} = \mathbf{0}$ for all i and j.

The RFID tag environment shown in Fig. 1 suggests that k_n tags may fall within the reader range. Accordingly, k_n time-variant distances D_{in}, $i \in [1, k_n \geqslant 2]$ will be measured between the reader and the tags $\mathrm{T}_t(\chi_t, \mu_t, \zeta_t)$. Along with the measurements of Φ_n, the observation equations can thus be written as [15]

$$\begin{aligned} D_{1n} &= \sqrt{(\bar{\mu}_1 - y_n)^2 + (\bar{\chi}_1 - x_n)^2 + \zeta_1^2}\,, \\ &\ \vdots \\ D_{k_n n} &= \sqrt{(\bar{\mu}_{k_n} - y_n)^2 + (\bar{\chi}_{k_n} - x_n)^2 + \zeta_{k_n}^2}\,, \\ \Phi_n &= \Phi_n\,, \end{aligned}$$

where the coordinates $\bar{\chi}_i$, $\bar{\mu}_i$, and ζ_i belong to the ith detected tag which is one of the nested tags $\mathrm{T}_t(\chi_t, \mu_t, \zeta_t)$.

If to follow Fig. 1 and Fig. 2 and introduce the observation vector $\mathbf{z}_n = [\, z_{1n}\ \ldots\ z_{k_n n}\ z_{\phi n}\,]^T$, the nonlinear function vector $\mathbf{h}_n(\mathbf{x}_n) = [\, D_{1n}\ \ldots\ D_{k_n n}\ \Phi_n\,]^T$, and the measurement additive noise vector $\mathbf{v}_n = [\, v_{1n}\ \ldots\ v_{k_n n}\ v_{\phi n}\,]^T$, then the state observation equation can be written as

$$\mathbf{z}_n = \mathbf{h}_n(\mathbf{x}_n) + \mathbf{v}_n\,, \tag{5}$$

where $\mathbf{v}_n$ is white Gaussian with zero mean $E\{\mathbf{v}_n\} = \mathbf{0}$, the covariance $\mathbf{R} = E\{\mathbf{v}_n\mathbf{v}_n^T\}$, and the properties $E\{\mathbf{v}_i\mathbf{w}_j^T\} = \mathbf{0}$ and $E\{\mathbf{v}_i\mathbf{e}_j^T\} = \mathbf{0}$ for all i and j.

In order to find an estimate $\hat{\mathbf{x}}_n = [\, \hat{x}_n\ \hat{y}_n\ \hat{\Phi}_n\,]$ of $\mathbf{x}_n$ using methods of linear filtering such as Kalman filtering, nonlinear functions in (1) and (5) are expanded to the first-order Taylor series as shown in [14, 15] to have the first-order extended state-space model

$$\mathbf{x}_n \;=\; \mathbf{F}_n\mathbf{x}_{n-1} + \bar{\mathbf{u}}_n + \tilde{\mathbf{e}}_n + \tilde{\mathbf{w}}_n\,, \tag{6}$$

$$\mathbf{z}_n \;=\; \mathbf{H}_n\mathbf{x}_n + \bar{\mathbf{z}}_n + \mathbf{v}_n\,, \tag{7}$$

where $\bar{\mathbf{u}}_n = \mathbf{f}_n(\hat{\mathbf{x}}_{n-1}, \mathbf{u}_n, \mathbf{0}, \mathbf{0}) - \mathbf{F}_n\hat{\mathbf{x}}_{n-1}$ and $\bar{\mathbf{z}}_n = \mathbf{h}_n(\hat{\mathbf{x}}_n^-) - \mathbf{H}_n\hat{\mathbf{x}}_n^-$ are known, $\tilde{\mathbf{e}}_n = \mathbf{E}_n\mathbf{e}_n$, and $\tilde{\mathbf{w}}_n = \mathbf{W}_n\mathbf{w}_n$. The Jacobian matrices $\mathbf{F}_n$, $\mathbf{W}_n$, $\mathbf{E}_n$, and $\mathbf{H}_n$ are given by $\mathbf{F}_n = \mathbf{W}_n$,

$$\mathbf{F}_n = \begin{bmatrix} 1 & 0 & -d_n\sin(\hat{\Phi}_{n-1} + \frac{1}{2}\phi_n) \\ 0 & 1 & d_n\cos(\hat{\Phi}_{n-1} + \frac{1}{2}\phi_n) \\ 0 & 0 & 1 \end{bmatrix}, \quad (8)$$

$$\mathbf{E}_n = \frac{1}{2b}\begin{bmatrix} be_{\mathrm{cn}} + d_n e_{\mathrm{sn}} & be_{\mathrm{cn}} - d_n e_{\mathrm{sn}} \\ be_{\mathrm{sn}} - d_n e_{\mathrm{cn}} & be_{\mathrm{sn}} + d_n e_{\mathrm{cn}} \\ -2 & 2 \end{bmatrix} \quad (9)$$

$$\mathbf{H}_n = \begin{bmatrix} \frac{\hat{x}_n^- - \bar{\chi}_1}{\nu_{1n}} & \frac{\hat{y}_n^- - \bar{\mu}_1}{\nu_{1n}} & 0 \\ \vdots & \vdots & \vdots \\ \frac{\hat{x}_n^- - \bar{\chi}_{k_n}}{\nu_{(k_n n)}} & \frac{\hat{y}_n^- - \bar{\mu}_{k_n}}{\nu_{(k_n n)}} & 0 \\ 0 & 0 & 1 \end{bmatrix}, \quad (10)$$

where $e_{\mathrm{cn}} = \cos\left(\hat{\Phi}_n^- + \frac{\phi_n}{2}\right)$, $e_{\mathrm{sn}} = \sin\left(\hat{\Phi}_n^- + \frac{\phi_n}{2}\right)$, and $\nu_{in} = \sqrt{(\bar{\mu}_i - \hat{y}_n^-)^2 + (\bar{\chi}_i - \hat{x}_n^-)^2 + \zeta_i^2}$. The zero mean noise vectors $\tilde{\mathbf{w}}_n$ and $\tilde{\mathbf{e}}_n$ have the covariances, $\tilde{\mathbf{Q}}_n = \mathbf{F}_n\mathbf{Q}\mathbf{F}_n^T$ and $\tilde{\mathbf{L}}_n = \mathbf{E}_n\mathbf{L}\mathbf{E}_n^T$. More detail about this model can be found in [14, 15].

Provided the estimates $\hat{\mathbf{x}}_n$ and $\hat{\mathbf{x}}_n^-$, the prior estimation error and estimation error can be found as, respectively,

$$\mathbf{P}_n^- = E\{(\mathbf{x}_n - \hat{\mathbf{x}}_n^-)(\mathbf{x}_n - \hat{\mathbf{x}}_n^-)^T\}, \quad (11)$$

$$\mathbf{P}_n = E\{(\mathbf{x}_n - \hat{\mathbf{x}}_n)(\mathbf{x}_n - \hat{\mathbf{x}}_n)^T\} \quad (12)$$

to be further minimized by choosing a proper estimator and optimizing the environment and UHF RFID network structure.

To estimate the object location and heading, we use the EFIR filter which pseudo code is given in Tab. 1. It has been shown in [14] that this filter is more robust than the EKF in real world under the uncertainties and unknown noise statistics.

3 Network Optimization

The localization accuracy can be increased if to optimize parameters of the scheme and environment. Most generally, we wish to minimize $\mathbf{P}_n$ (12) by setting optimally M parameters α_r, $r \in [1, M]$ as follows. Provided an EFIR estimate $\hat{\mathbf{x}}_n$ of the object state $\mathbf{x}_n$ over the UHF RFID tag network, the estimation error $\mathbf{P}_n$ can be minimized by setting α_i, $i \in M$, optimal parameters obtained by solving the optimization problem:

$$(\alpha_1^{\mathrm{opt}}, ..., \alpha_M^{\mathrm{opt}}) = \underset{\alpha_1,...,\alpha_M}{\arg\min}[\mathrm{tr}\,\mathbf{P}_n(\alpha_1, ..., \alpha_M)], \quad (13)$$

Table 1: EFIR Filtering Algorithm Code

	Input: $\mathbf{z}_n, \mathbf{y}_n, K, N$
1:	**for** $n = N-1 : M$ **do**
2:	$m = n - N + 1, \quad s = m + K - 1$
3:	$\tilde{\mathbf{x}}_s = \begin{cases} \mathbf{y}_s, & \textbf{if } s < N-1 \\ \hat{\mathbf{x}}_s, & \textbf{if } s \geqslant N-1 \end{cases}$
4:	$\mathbf{G}_s = \mathbf{I}$
5:	**for** $l = m + K : n$ **do**
6:	$\tilde{\mathbf{x}}_l^- = \mathbf{f}_l(\tilde{\mathbf{x}}_{l-1}, \mathbf{u}_l, \mathbf{0}, \mathbf{0})$
7:	$\mathbf{G}_l = [\mathbf{H}_l^T\mathbf{H}_l + (\mathbf{F}_l\mathbf{G}_{l-1}\mathbf{F}_l^T)^{-1}]^{-1}$
8:	$\mathbf{K}_l = \mathbf{G}_l\mathbf{H}_l^T$
9:	$\tilde{\mathbf{x}}_l = \tilde{\mathbf{x}}_l^- + \mathbf{K}_l[\mathbf{z}_l - \mathbf{h}_l(\tilde{\mathbf{x}}_l^-)]$
10:	**and for**
11:	$\hat{\mathbf{x}}_n = \tilde{\mathbf{x}}_n$
12:	**and for**
	Output: $\hat{\mathbf{x}}_n$

where $\mathrm{tr}\,\mathbf{P}_n$ is the trace of $\mathbf{P}_n$.

In unbiased FIR filtering [18], minimizing $\mathbf{P}_n$ means minimizing the generalized noise power gain (GNPG) given by line 7 in Table 1,

$$\mathbf{G}_n = [\mathbf{H}_n^T\mathbf{H}_n + (\mathbf{F}_n\mathbf{G}_{n-1}\mathbf{F}_n^T)^{-1}]^{-1}. \quad (14)$$

Because $\mathbf{G}_{n-1}$ is given and matrix $\mathbf{F}_n$ depends neither on the network nor on environment, the minimization of (14) can be achieved by maximizing the product $\mathbf{H}_n^T\mathbf{H}_n$. For $\mathbf{H}_n$ given by (10), the product $\mathbf{H}_n^T\mathbf{H}_n$ becomes

$$\mathbf{H}_n^T\mathbf{H}_n = \begin{bmatrix} \sum_{i=1}^{k_n}\frac{\Delta_{xi}^2}{\nu_i^2} & \sum_{i=1}^{k_n}\frac{\Delta_{xi}\Delta_{yi}}{\nu_i^2} & 0 \\ \vdots & \vdots & \vdots \\ \sum_{i=1}^{k_n}\frac{\Delta_{yi}\Delta_{xi}}{\nu_i^2} & \sum_{i=1}^{k_n}\frac{\Delta_{yi}^2}{\nu_i^2} & 0 \\ 0 & 0 & 1 \end{bmatrix}, \quad (15)$$

where $\Delta_{xi} = \hat{\mathbf{x}}_n^- - \bar{\chi}_i$, $\Delta_{yi} = \hat{\mathbf{y}}_n^- - \bar{\mu}_i$, and $\nu_i^2 = \Delta_{xi}^2 + \Delta_{yi}^2 + \zeta_i^2$. Note that all of the components of (15) must be maximized in order to minimize $\mathbf{P}_n$. Below, we analyse factors affecting the localization accuracy.

UHF tag optimization: The UHF RFID tag chip design is an important step in the design of the whole RFID system. The tag parameters influence antenna gain and impedance which, in turn, determine tag resonance, peak range, and bandwidth. A comprehensive analysis of the UHF tag chip design and optimization is given in [7] and we notice that the optimization must be provided for each particular tag design.

RSSI vs. distance: Effective peak-distances between the reader and reference tags are key factors affecting an accuracy of self-localization in the UHF RFID tag network. In diverse trilateration and hybrid schemes [11, 27, 28], the distances are measured via the RSSI which is a measurement of received radio signal power in terms of the ratio of measured power decibels (dB) to one milliwatt (mW). Based upon ESSI, the reader range is determined to provide reliable tag detection. All tags beyond the reader range deliver insufficient energy and cannot be identified with required error probability.

The Friis relation is commonly used to calculate the distance between the reader and the tag [25, 29],

$$P_r = P_t G_t G_r \frac{\lambda^2}{(4\pi)^2} \frac{1}{D^q}\,, \qquad (16)$$

where P_t and P_r are the transmitted and received powers, respectively, G_t and G_r are the gains of the tag antenna and the reader antenna, respectively, λ is the wavelength, D is the distance between tag and reader, and q is the signal strength exponent, which describes the influence of the transmission medium and which is equal to two, $q = 2$, for free space propagation [30].

It has been shown in [29] that, for $q = 2$, (16) leads to a relation between RSSI and D which has the following engineering form of

$$\mathrm{RSSI} = 32.4\,\mathrm{dB} + 20\log\left(\frac{f}{1\,\mathrm{GHz}}\right) - 20\log\left(\frac{D}{1\,\mathrm{m}}\right), \qquad (17)$$

Reader range: The reader range R is a key characteristic of any RFID tag system. The range can be determined using (16) as

$$R = \frac{\lambda}{4\pi}\eta\sqrt{\frac{P_t G_t G_r}{P_r}}\,, \qquad (18)$$

where the correction coefficient η requires an optimization for each particular design of the UHF RFID network or grid [23]. An example of the UHF RFID tag grid optimization is given in [24]. Optimization is provided here using the k nearest neighbor ($k-NN$) algorithm [31]. It has been shown that for RFID tag grids with equally spaces tags with a distance ρ, the optimal range can be defined periodically as $R = 1.25\rho + 0.5m$, $m = 0, 1...$, to minimize the MSE by the factor of about 2 with respect to the worst case of not optimal R.

Angle of arrival: In trilateration schemes, the angle of arrival ϑ_i of a signal from the ith tag to the reader (Fig. 3) is associated with the tag altitude ζ_i

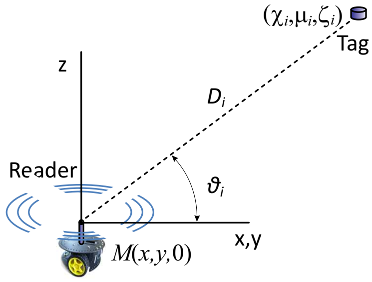

Figure 3: Angle of arrival ϑ_i of a signal from the ith tag to the reader.

(Fig. 2) measured with respect to the reader antenna altitude which is set to zero in this paper.

In order to minimize the localization error by ϑ_i via (13), let us maximize the $(1,1)$ component of matrix (15) by $\zeta_i^2 = D_i^2 \sin^2\vartheta_i^2$ as

$$\vartheta_i^{\mathrm{opt}} = \arg\max_{\vartheta_i} \sum_{i=1}^{k_n} \frac{\Delta_{xi}^2}{\Delta_{xi}^2 + \Delta_{yi}^2 + D_i^2 \sin^2\vartheta_i^2} \qquad (19)$$

$$\to \vartheta_i^{\mathrm{opt}} = 0\,.$$

By virtue of the fact that all of the values in (19) are positive, the maximization of the $(1,1)$ component as well as all other components in (15) is obtained by $\vartheta_i^{\mathrm{opt}} = 0$. That means that the optimal RFID network structure implies mounting all of the tags in the same horizontal plane with the reader antenna.

Tag orientation: For all kinds of passive RFID tags, the tag orientation affects the signal reading significantly. In order to provide sufficiently high RSSI level at any point of the indoor floorspace, 2D and 3D passive tag packages can be used. It has been shown in [32] that, when multiple tags are placed on same object, orthogonal orientations yield much higher detection probabilities than parallel orientations.

Viewing angle φ: A typical situation in RFID tagging is when the reader interacts with tags within some viewing angle $0 < \varphi < 2\pi$ as shown in Fig. 1. The *viewing angle* φ can be defined by a minimal segmental angle beginning with some tag to cover anticlockwise all other tags within the reader range (Fig. 1). Effect of φ on the localization accuracy is illustrated below.

Consider an object interacting with two RFID tags as shown in Fig. 4a. The measured distances D_1 and D_2 are coupled with the known tag's coordinates $(\chi_1 = 0, \mu_1)$ and $(\chi_2 = 0, \mu_2)$ and unknown object coordinates (x, y) by the relationships:

$$D_1^2 = x^2 + (y-\mu_1)^2\,, \quad D_2^2 = x^2 + (y-\mu_2)^2\,.$$

Suppose that measurements are provided with errors such that $D_{1,2} = D(1+\delta_{1,2})$, where δ_1 and δ_2 are

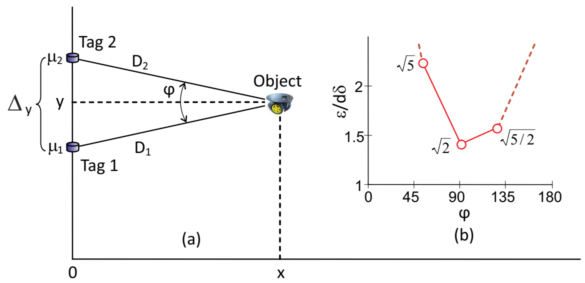

Figure 4: Example 1: Effect of a viewing angle φ on the localization accuracy.

fractional errors in the measured distances. In the worst case, one may suppose that $\delta_1 = -\delta_2$ and let $\delta_2 = \delta$. The coordinates x and y can now be represented with the deterministic components $\bar{x}$ and $\bar{y}$ and errors $\tilde{x}$ and $\tilde{y}$ as $x = \bar{x} + \tilde{x}$ and $y = \bar{y} + \tilde{y}$. Then solutions to (1) and (2) for $\bar{x}$ and $\bar{y}$ can be found as $\bar{x} = \sqrt{D^2 - (\mu_2 - \bar{y})^2}$ and $\bar{y} = (\mu_2 + \mu_1)/2$. Taking into account that $\mu_2 - \bar{y} = \Delta_y/2$, errors $\tilde{x}$ and $\tilde{y}$ can be found to be

$$\tilde{x} = \left(1 - \frac{4D^2}{\Delta_y^2}\right)\frac{D^2\delta^2}{2\bar{x}}, \quad \tilde{y} = -D^2\frac{2\delta}{\Delta_y}.$$

If we further introduce the viewing angle $\varphi = 2\bar{\varphi}$ via $\tan\bar{\varphi} = \Delta_y/2\bar{x}$ and substitute $D^2 = \bar{x}^2(1 + \tan^2\bar{\varphi})$, we can find the localization error $\varepsilon = \sqrt{\tilde{x}^2 + \tilde{y}^2}$ in the form of

$$\varepsilon = \bar{x}\delta\frac{1 + \tan^2\bar{\varphi}}{\tan\bar{\varphi}}\sqrt{1 + \frac{\delta^2}{4\tan^2\bar{\varphi}}},$$

which indicates that $\varphi = 0$ and $\varphi = \pi$ make ε infinite and that ε minimizes by

$$\varphi^{\text{opt}} = \arg\min_{\varphi} \bar{x}\delta\frac{1 + \tan^2\bar{\varphi}}{\tan\bar{\varphi}}\sqrt{1 + \frac{\delta^2}{4\tan^2\bar{\varphi}}}$$

$$\to \varphi^{\text{opt}} \cong \frac{\pi}{2} \quad (20)$$

More specifically, we arrive at a plot (Fig. 4b), which shows that a minimal $\varepsilon = d\delta\sqrt{2}$ corresponds to $\varphi = 90°$. Around this point, we have $\varepsilon = d\delta\sqrt{5}$ for $\varphi \cong 53°$ and $\varepsilon = d\delta\sqrt{5/2}$ for $\varphi \cong 126°$. This example suggests that the viewing angle φ should be set optimally in order to minimize the localization error.

Tag read density: Provided φ_{opt}, the localization error can further be reduced by increasing the tag read density, which is the number of tags k_n that can be read at once by the reader. Figure 5 demonstrates reduction of the localization RMSE by k_n within the optimal viewing angle $\varphi^{\text{opt}} = 90°$ using the EKF and

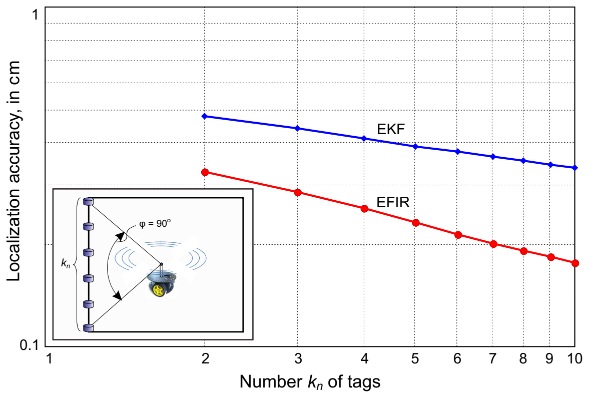

Figure 5: RMSE reduction by the number k_n of the tags for $\varphi_{\text{opt}} = 90°$ using the EKF and EFIR filter.

EFIR filter. The tags were placed equidistantly on the left wall of the room and their number varied from 2 to 10. As can be seen, both the EKF and EFIR filter improve the localization accuracy by increased k_n, but the EFIR filter demonstrates higher accuracy.

4 Conclusions

An analysis of factor affecting self-localization in UHF RFID tag-nested navigation networks has shown that the localization accuracy can be increased by the factor of several times, if to optimize the design and the environment. Such an optimization can make optimal estimators more efficient.

This work was supported by the Royal Academy of Engineering under the Newton Research Collaboration Programme NRCP/1415/140.

References:

[1] H. D. Chon, S. Jun, H. Jung, and S. W. An, "Using RFID for accurate positioning," *J. Global Positioning Syst.*, vol. 3, no. 1/2, pp. 32-39, 2004.

[2] S. Park and S. Hashimoto, "Autonomous Mobile Robot Navigation Using Passive RFID in Indoor Environment", *IEEE Transactions on Industrial Electronics*, vol. 56, no. 7, pp. 2366–2373 Jul. 2009.

[3] T. Sanpechuda and L. Kovavisaruch, "A review of RFID localization: Applications and techniques," in *Proc. 5th Int. Conf. Elect. Eng./Electron., Comput., Telecommun. Inf. Technol.*, May 2008, pp. 769772.

[4] J. Zhou and J. Shi, "RFID localization algorithms and applicationsa review," *J. Intell. Manuf.*, vol. 20, no. 6, pp. 695-707, Dec. 2009.

[5] F. Viani, P. Rocca, G. Oliveri, D. Trinchero, and A. Massa, "Localization, tracking, and imaging of tar-

gets in wireless sensor networks: An invited review," *Radio Science*, vol. 46, no. RS5002, pp. 1–12, 2011.

[6] ECPglobal Gen2 (ISO 18000-6C) UHF standard.

[7] K. V. S. Rao, P. V. Nikitin, and S. F. Lam, Antenna design for UHF RFID tags: a review and a practical application, *IEEE Trans. on Antennas and Propagation*, vol. 53, no. 12, pp. 3870–3876, Dec. 2005.

[8] S. S. Saab and Z. S. Nakad, "A standalone RFID indoor positioning system using passive tags," *IEEE Trans. on Industr. Electron.*, vol. 58, no. 5, pp. 1961–1970, May 2011.

[9] U, Klee, T. Gehrig and J. McDonough, "Kalman filters for time delay of arrival-based source localization," *EURASIP Journal on Applied Signal Process.*, vol. 2006, pp. 1–15, Jan. 2006.

[10] E. DiGiampaolo and F. Martinelli, "A passive UHF-RFID system for the localization of an indoor autonomous vehicle," *IEEE Trans. on Industr. Electron.*, vol. 59, no. 10, pp, 3961–3970, Oct. 2012.

[11] S. Park and H. Lee, "Self-recognition of vehicle position using UHF passive RFID tags," *IEEE Trans. on Industr. Electron.*, vol. 60, no. 1, pp. 226–234, Jan. 2013.

[12] D. Hahnel, W. Burgard, D. Fox, K. Fishkin, and M. Philipose, "Mapping and localization with RFID technology," in Proc. *IEEE Int. Conf on Robotics and Automation*, vol. 1, pp. 1015–1020, 2004.

[13] E. DiGiampaolo and F. Martinelli, "Mobile robot localization using the phase of passive UHF-RFID signals," *IEEE Trans. on Industr. Electron.*, vol. 61, no. 1, pp. 365–376, Jan. 2014.

[14] J. Pomarico-Franquiz, M. Granados-Cruz, and Y. S. Shmaliy, "Self-localization over RFID tag grids excess channels using extended filtering techniques," *IEEE J. of Selected Topics in Signal Process.*, vol. 9, no. 2, pp. 229–238, Mar. 2015.

[15] J. Pomarico-Franquiz and Y. S. Shmaliy, "Accurate self-localization in RFID tag information grids using FIR filtering," *IEEE Trans. Industrial Informatics*, vol. 10, no. 2, pp. 1317–1326, May 2014.

[16] J. Pomarico-Franquiz, S. Khan, and Y. S. Shmaliy, "Combined extended FIR/Kalman filtering for indoor robot localization via triangulation," *Measurement*, vol. 50, pp. 236–242, Apr. 2014.

[17] Y. S. Shmaliy, "Suboptimal FIR filtering of nonlinear models in additive white Gaussian noise," *IEEE Trans. Signal Process.*, vol. 60, no. 10, pp. 5519–5527, Oct. 2012.

[18] Y. S. Shmaliy, "An iterative Kalman-like algorithm ignoring noise and initial conditions," *IEEE Trans. Signal Process.*, vol. 59, no. 6, pp. 2465–2473, Jun. 2011.

[19] Y. S. Shmaliy, "Unbiased FIR filtering of discrete time polynomial state space models," *IEEE Trans. on Signal Process.*, vol. 57, no. 4, pp. 1241–1249, Apr. 2009.

[20] A. H. Jazwinski, *Stochastic Processes and Filtering Theory*, New York: Academic, 1970.

[21] W. H. Kwon and S. Han, *Receding Horizon Control: Model Predictive Control for State Models*. London: Springer, 2005.

[22] J. M. Pak, C. K. Ahn, Y. S. Shmaliy, and M. T. Lim, "Improving reliability of particle filter-based localization in wireless sensor networks via hybrid particle/FIR filtering," *IEEE Trans. Industrial Informatics*, vol. 11, no. 5, pp. 1089–1098, Oct. 2015.

[23] P. Sorrells, "Optimizing read range in RFID systems," *Design Feature*, pp. 173–184, 7 Dec. 2000.

[24] S. Han, J. Kim, C.-H. Park, H.-C. Yoon, and J. Heo, "Optimal detection range of RFID tag for RFID-based positioning system using the k-NN algorithm", *Sensors*, vol. 9, pp. 4543–4558, 2009.

[25] A. W. Reza, T. T. Rui, and A. S. M. Kausar, "An optimized indoor RFID positioning system using 3D mobility pattern," *Advances in Electrical and Computer Engineering*, vol. 14, no. 2, 2014.

[26] L. Ma, H. Chen, K. Hu, and Y. Zhu, "Hierarchical artificial bee colony algorithm for RFID network planning pptimization," *The Scientific World Journal*, vol. 2014, Art. ID 941532, 21 P, 2014.

[27] Y. C. Chen and J. H. Chou, "Mobil robot localization by RFID method," in Proc. *7th Int. Conf. Digital Commun. (ICDT-2012)*, 2012, pp. 33-38.

[28] R. Krigslund, P. Popovski, G. F. Pedersen, and K. Olesen, "Interference helps to equalize the read range and reduce false positives of passive RFID tags," *IEEE Trans. on Industr. Electron.*, vol. 59, no. 12, pp. 4821–4830, Dec. 2012.

[29] K. G. Tan, A. W. Reza, and C. P. Tan, "Object tracking utilizing square grid RFID reader antenna network," *Journal of Electromagnetic Waves and Applications*, vol. 22, no. 1, pp. 27–38, 2008.

[30] S. Y. Seidel and T. S. Rappaport, "914 MHz path loss prediction models for indoor wireless communications in multifloored buildings," *IEEE Transactions on Antennas and Propagation*, vol. 40, pp. 207217, 1992.

[31] L. M. Ni, Y. Liu, Y. C. Lau, and A. P. Patil, "LANDMARC: indoor location sensing using active RFID," *Wireless Networks*, vol. 10, pp. 701–710, 2004.

[32] L. Bolotnyy and G. Robins, "The Case for Multi-Tag RFID Systems, in *Proc. IEEE Int. Conf. on Wireless Algorithms, Systems and Applications (WASA 2007)*, Chicago, Aug. 2007, pp. 174–186.